

## An Upwind Differencing Scheme for the Equations of Ideal Magnetohydrodynamics

M. BRIO AND C. C. WU

*Department of Physics, University of California,  
Los Angeles, California 90024*

Received June 21, 1985; revised May 15, 1987

Recently, upwind differencing schemes have become very popular for solving hyperbolic partial differential equations, especially when discontinuities exist in the solutions. Among many upwind schemes successfully applied to the problems in gas dynamics, Roe's method stands out for its relative simplicity and clarity of the underlying physical model. In this paper, an upwind differencing scheme of Roe-type for the MHD equations is constructed. In each computational cell, the problem is first linearized around some averaged state which preserves the flux differences. Then the solution is advanced in time by computing the wave contributions to the flux at the cell interfaces. One crucial task of the linearization procedure is the construction of a Roe matrix. For the special case  $\gamma = 2$ , a Roe matrix in the form of a mean value Jacobian is found, and for the general case, a simple averaging procedure is introduced. All other necessary ingredients of the construction, which include eigenvalues, and a complete set of right eigenvectors of the Roe matrix and decomposition coefficients are presented. As a numerical example, we chose a coplanar MHD Riemann problem. The problem is solved by the newly constructed second-order upwind scheme as well as by the Lax Friedrichs, the Lax-Wendroff, and the flux-corrected transport schemes. The results demonstrate several advantages of the upwind scheme. In this paper, we also show that the MHD equations are nonconvex. This is a contrast to the general belief that the fast and slow waves are like sound waves in the Euler equations. As a consequence, the wave structure becomes more complicated; for example, compound waves consisting of a shock and attached to it a rarefaction wave of the same family can exist in MHD. © 1988 Academic Press, Inc.

### I. INTRODUCTION

In recent years upwind differencing schemes have become very popular for solving hyperbolic partial differential equations with discontinuous solutions. This popularity is mainly due to the robustness of the schemes, the availability of an underlying physical model, and their ability of achieving high resolution of stationary discontinuities. A general discussion of the upwind differencing schemes can be found in a review article by Harten, *et al.* [1]. An extensive comparison between the upwind schemes and other numerical schemes on some two-dimensional hydrodynamical problems with strong shocks has recently been reported by Woodward and Colella [2].

In this paper an upwind differencing scheme for the equations of ideal

magnetohydrodynamics (MHD) is presented. The MHD equations form a non-strictly hyperbolic system. In one-dimensional case, the Jacobian is a  $7 \times 7$  matrix and up to 5 out of the 7 eigenvalues may coincide. In addition, as we will show in Section 6 of the paper, the MHD equations are nonconvex. As a consequence, the wave structure is more complicated than for the Euler equations. For example, one can have a compound wave which consists of a shock and attached to it a rarefaction wave of the same family. This is a contrast to the usual belief that the magnetosonic waves are like sound waves in the Euler equations.

Because of the complexity of the MHD equations, we have constructed the scheme by using Roe's linearization procedure [3]. We have also attempted to apply other upwind schemes which are based on nonlinear approximations of the system of conservation laws, such as Godunov's [4] or Osher's [5] schemes, but construction becomes very involved, since the MHD Riemann problem is complicated and has not yet been fully resolved.

The plan of this paper is as follows: In Section 2, MHD equations are defined. In Section 3, we present a brief account of Roe's method. One critical task in his procedure is the construction of a Roe matrix. For the MHD equations, this is presented in Section 4. For the special case  $\gamma = 2$ , we have constructed a Roe matrix due to the existence of a mean value Jacobian. However, for the general  $\gamma$  case, we have not succeeded in constructing a Roe matrix. Instead, a simple averaging procedure is introduced. The eigenvalues, eigenvectors, and decomposition coefficients, which are necessary ingredients for the construction of the scheme, are also listed in this section. Since the underlying Riemann problem is linear, one has to have a complete set of right eigenvectors which are well defined for all values of parameters. In this paper a complete set of independent eigenvectors is provided. Section 5 shows some numerical experiments for a one-dimensional MHD Riemann problem. The problem is solved by using a second-order upwind scheme, and the results are compared with those obtained by standard difference schemes, such as the Lax-Friedrichs scheme, the Lax-Wendroff scheme with Lapidus-type viscosity, and the flux-corrected transport (FCT) scheme. The experiments indicate several advantages of the upwind scheme. Besides, the model problem demonstrates the existence of a compound wave for the MHD equations, which consists of a shock followed by a rarefaction wave of the same family. Also in this section, we discuss the solution of a high Mach number Riemann problem by the upwind scheme and compare it with the exact analytical solution.

In Section 6, we prove that the MHD equations are nonconvex. By using the complete set of right eigenvectors constructed in this paper, we will show that as the transverse magnetic field goes through zero, the slow (fast) characteristic field becomes degenerate if the sound speed is greater (less) than the Alfvén speed. As a remark, one can check that the usually used set of right eigenvectors for the MHD equations, for example, those given by Jeffrey and Taniuti [6], is not complete. The difference between our set and theirs is in normalization. By using their set, it follows that fast and slow characteristic fields are genuinely nonlinear, see Theorem E.1 in Jeffrey and Taniuti [6].

## II. MHD EQUATIONS

The MHD equations characterize the flow of a conducting fluid in the presence of magnetic field. They represent coupling of the fluid dynamical equations with Maxwell's equations of electrodynamics. By neglecting displacement current, electrostatic forces, effects of viscosity, resistivity, and heat conduction, one obtains the following ideal MHD equations [6]:

$$\rho_t + \nabla \cdot (\rho \mathbf{u}) = 0, \quad (1)$$

$$(\rho \mathbf{u})_t + \nabla \cdot (\rho \mathbf{u} \mathbf{u} + \tilde{P}^* \mathbf{I} - \mathbf{B} \mathbf{B}) = 0, \quad (2)$$

$$\mathbf{B}_t + \nabla \cdot (\mathbf{u} \mathbf{B} - \mathbf{B} \mathbf{u}) = 0, \quad (3)$$

$$E_t + \nabla \cdot ((E + P^*) \mathbf{u} - \mathbf{B}(\mathbf{B} \cdot \mathbf{u})) = 0, \quad (4)$$

with the additional requirement that  $\nabla \cdot \mathbf{B} = 0$ , which is satisfied in the initial value problem if it is satisfied initially. In the above equations the following notations are used:  $\rho$  for density,  $\mathbf{u}$  for velocity,  $\mathbf{B}$  for magnetic field,  $P$  for static pressure,  $P^*$  for full pressure,  $P^* = P + \frac{1}{2} \|\mathbf{B}\|^2$ ,  $E$  for energy,  $E = \frac{1}{2} \rho \|\mathbf{u}\|^2 + P/(\gamma - 1) + \frac{1}{2} \|\mathbf{B}\|^2$ , and  $\gamma$  for the ratio of specific heats. Furthermore, we have chosen units such that factors of  $4\pi$  and  $c$  do not appear in Eqs. (1)–(4).

The above system is hyperbolic, its Jacobian has real eigenvalues and a complete set of right eigenvectors [6, 7]. However, it is not a strictly hyperbolic system since the eigenvalues may coincide. (For a strictly hyperbolic system, all eigenvalues are distinct.) Also the system is nonconvex, since there are fields which cannot be characterized as either linearly degenerate or genuinely nonlinear. This will be discussed in Section 6.

## III. REVIEW OF ROE CONSTRUCTION

Let us discretize space and time as  $x_i = i \Delta x$  and  $t_n = n \Delta t$ , as shown in Fig. 1, and denote by  $v_i^n$  a piecewise linear approximation to the exact solution of the following system of conservation laws:

$$U_t + F(U)_x = 0, \quad (5)$$

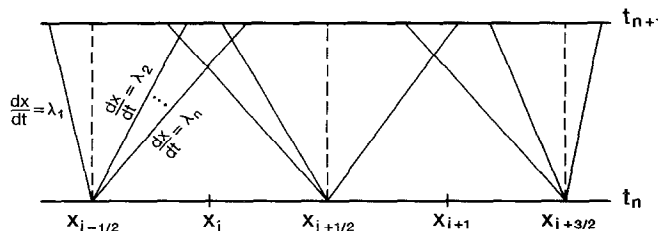


FIG. 1. Piecewise linear initial value problem which is integrated to advance piecewise constant initial data  $v_i^n$  from time  $t_n$  to  $t_{n+1}$ .

where  $U$  is a vector which represents the variables and  $F(U)$  represents the flux vector.

The difference approximation to (5) can be written in conservation form as

$$\frac{v_i^{n+1} - v_i^n}{\Delta t} + \frac{f_{i+1/2} - f_{i-1/2}}{\Delta x} = 0, \quad (6)$$

where  $f_{i+1/2}$  is called numerical flux. A numerical scheme in conservation form is called an upwind scheme if it reduces to the method of characteristics when applied to linear system and also satisfies the entropy condition [1].

Among many upwind schemes successfully applied to the hyperbolic problems with discontinuous solutions, Roe's method stands out by its simplicity and clarity of the underlying physical model. In each computational cell the problem is linearized around some averaged state, so that the flux difference is preserved in each cell. The solution is then advanced in time by computing explicitly the wave contributions to the flux at the cell interfaces. This is done by solving an initial value problem with the step function as its initial data (Riemann problem) for the linear system. The time step size is restricted as usual by the CFL condition that waves do not travel more than one computational cell in one time step. The details are as follows:

In the first step of the Roe construction, the exact system (5) is approximated in each computational cell  $(x_i, x_{i+1}) \times (t_n, t_{n+1})$  by a linear system

$$U_t + G(U)_x = 0, \quad (7)$$

where

$$G(U) = F_i + A_{i+1/2}(U - v_i^n), \quad F_i = F(U_i). \quad (8)$$

Here the Roe matrix  $A_{i+1/2}$  is such that

$$(1) \quad F_{i+1} - F_i = A_{i+1/2}(U_{i+1} - U_i) \quad \text{for any } U_i \text{ and } U_{i+1}, \quad (9A)$$

$$(2) \quad A_{i+1/2} \text{ has real eigenvalues and a complete set of right eigenvectors,} \quad (9B)$$

$$(3) \quad A_{i+1/2}(U_{i+1}, U_i) \rightarrow A(U_0) = \left. \frac{\partial F}{\partial U} \right|_{U=U_0} \text{ as } U_{i+1} \text{ and } U_i \rightarrow U_0. \quad (9C)$$

Note that by the property (9A)  $G(U)$  can be written equivalently as

$$G(U) = F_{i+1} + A_{i+1/2} \cdot (U - v_{i+1}^n). \quad (10)$$

In the second step of the construction, we solve the linear Riemann problem for the system (7) with the initial data defined as  $v_i^n$  for  $x < x_{i+1/2}$  and  $v_{i+1}^n$  for  $x > x_{i+1/2}$ . Then the flux  $f_{i+1/2}$  is defined as

$$f_{i+1/2} = G(v_{i+1/2}). \quad (11)$$

Here  $v_{i+1/2}$  denotes the solution of the above Riemann problem at  $x = x_{i+1/2}$ . The linear Riemann problem can easily be solved by decomposing the system (7) into a set of uncoupled scalar linear equations. It is done by multiplying the system (7) by the left eigenvectors of the matrix  $A_{i+1/2}$  and solving each scalar linear equation exactly.

This implies that for  $\Delta t \leq \Delta x / \max_{k,i} |\lambda_k^{i+1/2}|$ ,  $v_{i+1/2}$  is given by

$$v_{i+1/2} = v_i + \sum_{k, \lambda_k^{i+1/2} < 0} C_k^{i+1/2} R_k^{i+1/2}, \quad (12)$$

where  $\lambda_k^{i+1/2}$  and  $R_k^{i+1/2}$  represent the eigenvalue and the corresponding eigenvector of  $A_{i+1/2}$ .  $C_k^{i+1/2}$  is the decomposition coefficient of  $(v_{i+1} - v_i)$  in the right eigenvector space as defined by the following relation

$$v_{i+1} - v_i = \sum_k C_k^{i+1/2} R_k^{i+1/2}. \quad (13)$$

Substituting  $v_{i+1/2}$  in (11) by expression (12) gives

$$f_{i+1/2} = F_i + \sum_{k, \lambda_k^{i+1/2} < 0} \lambda_k^{i+1/2} C_k^{i+1/2} R_k^{i+1/2}. \quad (14)$$

By property (9A), it is equivalent to

$$\begin{aligned} f_{i+1/2} &= F_{i+1} - \sum_{k, \lambda_k^{i+1/2} < 0} \lambda_k^{i+1/2} C_k^{i+1/2} R_k^{i+1/2} \\ &= \frac{1}{2} (F_i + F_{i+1}) - \frac{1}{2} \sum_k |\lambda_k^{i+1/2}| C_k^{i+1/2} R_k^{i+1/2}. \end{aligned} \quad (15)$$

In the following some special properties of the Roe scheme are presented. First, property (9A) together with the Rankine-Hugoniot jump relations, implies that the speed of the discontinuity and the jump through the discontinuity are, respectively, some eigenvalue and eigenvector of the matrix  $A_{i+1/2}$ . This implies that stationary discontinuities are steady solutions of the numerical scheme. Second, since the scheme is based on a linear decomposition of the characteristic fields, one can apply different numerical schemes for each field. For example, one can use artificial compression on linearly degenerate fields in order to prevent their spreading [8] or, in the multiple time scale problems, treat some fields implicitly, so that a larger time step can be used. Third, the scheme is non-oscillatory in the sense that no new extrema is created for the linear systems or a single nonlinear conservation law [8]. The above construction gives a difference approximation of first-order accuracy and may admit entropy violating shocks. For practical purposes, the scheme is usually extended to second order with some entropy fix, see for example Harten [8] or Osher [9]. Also, upwind schemes can be applied on adaptive mesh [10], and in non-Cartesian coordinates [9]. Extensions to multi-dimensional geometries can be done with or without dimensional splitting [9].

We summarize the steps in constructing a Roe-type scheme:

- (1) Obtain matrix  $A_{i+1/2}$  as defined by (9A)–(9C).
- (2) Compute the eigenvalues  $\lambda_k^{i+1/2}$  and the eigenvectors  $R_k^{i+1/2}$  of  $A_{i+1/2}$ .
- (3) Calculate decomposition coefficients  $C_k^{i+1/2}$  as defined by (13).
- (4) Compute  $f_{i+1/2}$  and obtain  $v_i^{n+1}$  by (6).

In the next section we will show these steps in building an upwind scheme for the MHD equations.

#### IV. ROE-TYPE SCHEME FOR THE MHD EQUATIONS

In this section we consider one-dimensional MHD equations which are obtained from the system (1)–(4) by assuming that all variables depend on  $x$  and  $t$  only. The resulting equations are:

$$\rho_t + (\rho u)_x = 0, \quad (16)$$

$$(\rho u)_t + (\rho u^2 + P^*)_x = 0, \quad (17)$$

$$(\rho v)_t + (\rho uv - B_x B_v)_x = 0, \quad (18)$$

$$(\rho w)_t + (\rho uw - B_x B_w)_x = 0, \quad (19)$$

$$(B_y)_t + (B_y u - B_x v)_x = 0, \quad (20)$$

$$(B_z)_t + (B_z u - B_x w)_x = 0, \quad (21)$$

$$E_t + ((E + P^*)u - B_x(B_x u + B_y v + B_z w))_x = 0. \quad (22)$$

$B_x \equiv \text{const}$ ,  $u$ ,  $v$ , and  $w$  are three components of the velocity field, and the rest of the notations are as in Section II.

##### IV.1. Matrix $A_{i+1/2}$

The Jacobian of the system (16)–(22) is

$$A = \begin{pmatrix} 0 & 1 & 0 & 0 & 0 & 0 & 0 \\ \frac{\gamma-3}{2}u^2 + \frac{\gamma-1}{2}(v^2 + w^2) & (3-\gamma)u & (1-\gamma)v & (1-\gamma)w & (2-\gamma)B_x & (2-\gamma)B_z & (\gamma-1)P^* \\ -uw & v & u & 0 & -B_x & 0 & 0 \\ -vw & w & 0 & u & 0 & -B_x & 0 \\ -\frac{B_x}{\rho}u + \frac{B_y}{\rho}v & \frac{B_y}{\rho} & -\frac{B_x}{\rho} & 0 & u & 0 & 0 \\ -\frac{B_z}{\rho}u + \frac{B_x}{\rho}w & \frac{B_z}{\rho} & 0 & -\frac{B_x}{\rho} & 0 & u & 0 \\ \alpha_1 & \alpha_2 & \alpha_3 & \alpha_4 & \alpha_5 & \alpha_6 & \alpha_7 \end{pmatrix}, \quad (23)$$

where  $H = (E + P^*)/\rho$ , and

$$\begin{aligned}\alpha_1 &= -u \left( H \frac{\gamma-1}{2} (u^2 + v^2 + w^2) + \frac{B_x}{\rho} (B_x u + B_y v + B_z w) \right), \\ \alpha_2 &= H - B_x^2/\rho - (\gamma-1) u^2, \\ \alpha_3 &= (1-\gamma) uv - B_x B_y/\rho, \\ \alpha_4 &= (1-\gamma) uw - B_x B_z/\rho, \\ \alpha_5 &= (2-\gamma) B_y u - B_x v, \\ \alpha_6 &= (2-\gamma) B_z u - B_x w, \\ \alpha_7 &= \gamma u.\end{aligned}$$

For the special case  $\gamma=2$ , we are able to find matrix  $A_{i+1/2}$  as defined by (9A)–(9C) in the form of  $A(V_{i+1/2}(U_i, U_{i+1}))$ , with  $A$  a Jacobian matrix for the system (16)–(22) calculated at some average state  $V_{i+1/2}(U_i, U_{i+1})$ . In order to find  $V_{i+1/2}$ , one solves the following system of algebraic equations (see Eq. (9A)),

$$F(U_{i+1}) - F(U_i) = A(V_{i+1/2})(U_{i+1} - U_i), \quad (24)$$

where  $V_{i+1/2}(v_1, v_2, \dots, v_7)$  represents some averaged values of the components of  $U_i$  and  $U_{i+1}$ .  $U$  and  $F$  are as in the system (16)–(22); namely,

$$\begin{aligned}U &= (\rho, \rho u, \rho v, \rho w, B_x, B_y, B_z, E), \\ F &= (\rho u, \rho u^2 + P^*, \rho uv - B_x B_y, \rho uw - B_x B_z, \\ &\quad B_y u - B_x v, B_z u - B_x w, (E + P^*)u - B_x(B_x u + B_y v + B_z w)),\end{aligned}$$

and  $A$  is the Jacobian matrix (23). In addition, we require  $V_{i+1/2}$  to satisfy the following properties:

$$(1) \quad V_{i+1/2}(U_{i+1}, U_i) = V_{i+1/2}(U_i, U_{i+1}), \quad (25A)$$

$$(2) \quad V_{i+1/2} \text{ is continuous and } V_{i+1/2}(U, U) = U, \quad (25B)$$

$$(3) \quad V_{i+1/2} \text{ is such that eigenvalues of } A(V_{i+1/2}) \text{ are real.} \quad (25C)$$

Note that for the Euler equations, the matrix  $A_{i+1/2}$  constructed by Roe using his parametrization technique [3] is in the form of  $A(V_{i+1/2})$ . If one applies the above procedure to the Euler equations, the resulting  $V_{i+1/2}$  is unique and identical to the one constructed by Roe.

There are seven equations in (24). The first equation is satisfied automatically. Introducing  $\hat{u} = v_2/v_1$ ,  $\hat{v} = v_3/v_1$ , and  $\hat{w} = v_4/v_1$ , one can show that each of the next three equations represents geometrically a hyperboloid formed by revolution around the  $\hat{u}$  axis and two hyperbolic cylinders, respectively. It can be shown that they intersect at two points, but only one of which satisfies properties (25B) and (25C). The solution obtained is identical to the solution for the Euler equations:

$$\hat{u} = \frac{\langle \rho^{1/2} u \rangle}{\langle \rho^{1/2} \rangle}, \quad (26)$$

with similar expressions for  $\hat{v}$  and  $\hat{w}$ ;  $\langle \cdot \rangle$  denotes here the arithmetic average of values at  $i$  and  $i+1$ . Substituting them into the fifth equation of (24) gives, after some algebraic manipulations,

$$\frac{B_x}{\rho^*} \left( \frac{1}{v_1} - \frac{1}{\rho^*} \right) \Delta v + \left( \frac{v_5}{v_1} - \left\langle \frac{B_y}{\rho^{1/2}} \right\rangle \left\langle \rho^{1/2} \right\rangle \right) \Delta u = 0, \quad (27)$$

where  $\rho^*$  denotes the geometric average of  $\rho_i$  and  $\rho_{i+1}$ ,  $\Delta v = v_{i+1} - v_i$ ,  $\Delta u = u_{i+1} - u_i$ . Since we are looking for a solution which is valid for all values of  $U_{i+1}$  and  $U_i$ , (27) implies that

$$v_1 = \rho^* \quad (28)$$

$$v_5 = \frac{\langle B_y / \rho^{1/2} \rangle}{\langle \rho^{1/2} \rangle} \rho^*. \quad (29)$$

The next equation (number six) of (24) gives  $v_6$  similar to (29) if one replaces  $B_y$  by  $B_z$ . Finally, the last equation of (24) is linear in  $\hat{E}$  or  $\hat{H}$  and gives

$$\hat{H} = \frac{\langle \rho^{1/2} H \rangle}{\langle \rho^{1/2} \rangle}. \quad (30)$$

For general one-dimensional case ( $\gamma \neq 2$ ), the nonlinear algebraic system of Eq. (24) for variables  $V_{i+1/2}$  does not decouple as in the previous case ( $\gamma = 2$ ), and we are not able to solve it analytically. Neither do we succeed in finding an appropriate parameterization as suggested by Roe [3]. Instead, we have modified Roe's method by using a simple averaging scheme:  $A_{i+1/2}$  is defined as a Jacobian  $A(W_{i+1/2})$  with the  $W_{i+1/2}$  denoting some averaging function that satisfies properties (25A)–(25C). One can check that the averaging method satisfies the properties (9B) and (9C), but not (9A). Violation of property (9A) implies that the stationary discontinuities are no longer steady solutions of the resulting numerical scheme, but as was shown in [11], they still can be resolved with few grid points.

For the Euler equations and the MHD equations, if one uses an averaging function  $W_{i+1/2}$  such that the averaged density and the pressure have positive values, then all of the eigenvalues of  $A(W_{i+1/2})$  are real (property (25C)). One simple example for  $W$  is to take an arithmetic averaging of the density, velocity, magnetic field, and full pressure. Note that if instead of averaging the full pressure, one averages the energy variable, it may lead to a negative averaged pressure which is not allowed.

#### IV.2. Eigenvalues of the Jacobian $A$

The eigenvalues can be written in nondecreasing order as

$$u - c_f, \quad u - c_a, \quad u - c_s, \quad u, \quad u + c_s, \quad u + c_a, \quad u + c_f \quad (31)$$



where  $c_f$ ,  $c_a$ ,  $c_s$  are the fast, the Alfvén, and the slow characteristic speeds, respectively. They can be expressed as

$$c_a^2 = b_x^2, \quad (32)$$

$$c_{f,s}^2 = \frac{1}{2}((a^*)^2 \pm \sqrt{(a^*)^4 - 4a^2 b_x^2}), \quad (33)$$

with the notations

$$b_x = B_x/(\rho)^{1/2}, \quad b_y = B_y/(\rho)^{1/2}, \quad b_z = B_z/(\rho)^{1/2},$$

$$b^2 = b_x^2 + b_y^2 + b_z^2, \quad (a^*)^2 = (\gamma p + B^2)/\rho$$

and  $a$  is the sound speed which is given by

$$a^2 = \gamma p/\rho.$$

In Eq. (33) the plus sign is for the  $c_f$  and minus sign for the  $c_s$ .

There are two points where these eigenvalues may coincide:

(1) At  $B_x = 0$ ,  $c_s = c_a = 0$ , thus  $u$  is an eigenvalue of multiplicity 5.

(2) At  $B_y^2 + B_z^2 = 0$ ,  $c_f^2 = \max(a^2, b_x^2)$ , and  $c_s^2 = \min(a^2, b_x^2)$ . Therefore, for the case  $a^2 \neq b_x^2$ , either  $c_f^2 = b_x^2$  or  $c_s^2 = b_x^2$ , thus multiplicity of  $u \pm c_a$  is 2; and for the case  $a^2 = b_x^2$ ,  $c_f^2 = c_s^2 = b_x^2$  and the multiplicity of  $u \pm c_a$  is 3.

#### IV.3. Eigenvectors of $A$

In order to carry out Roe's linearization procedure, one requires the matrix  $A$  to have a complete set of right eigenvectors, so that it can be diagonalized and then one can proceed with the construction from Eq. (7) to Eq. (12). The following set of right eigenvectors is given by Jeffrey and Taniuti [3]

$$R_{u \pm c} = \begin{bmatrix} 1 \\ u \pm c \\ v \mp \frac{B_x B_y c}{\rho(c^2 - b_x^2)} \\ w \mp \frac{B_x B_z c}{\rho(c^2 - b_x^2)} \\ \frac{B_y c^2}{\rho(c^2 - b_x^2)} \\ \frac{B_z c^2}{\rho(c^2 - b_x^2)} \\ \frac{u^2 + v^2 + w^2}{2} + h \end{bmatrix}, \quad R_{u \pm c_a} = \begin{bmatrix} 0 \\ 0 \\ \mp B_z \operatorname{sgn}(B_x) \\ \pm B_y \operatorname{sgn}(B_x) \\ B_z/\rho^{1/2} \\ -B_y/\rho^{1/2} \\ g \end{bmatrix}, \quad R_u = \begin{bmatrix} 1 \\ u \\ v \\ w \\ 0 \\ 0 \\ \frac{u^2 + v^2 + w^2}{2} \end{bmatrix}, \quad (34)$$

where  $c$  is either  $c_f$  or  $c_s$ , and  $h$  and  $g$  are defined as

$$h = \frac{c^2}{\gamma - 1} \pm cu \mp \frac{B_x c (B_x v + B_z w)}{\rho(c^2 - b_v^2)} + \frac{\gamma - 2}{\gamma - 1} (c^2 - a^2),$$

$$g = \mp (B_z v \mp B_y w) \operatorname{sgn}(B_x).$$

However, near the points where either  $B_x = 0$  or  $B_y^2 + B_z^2 = 0$ , this set is not well defined and the matrix with these eigenvectors as its columns becomes singular. We construct a complete set by renormalizing the above eigenvectors. To find the normalizing factors, we examine the behavior of the eigenvectors (34) near these points.

(1) At  $B_x = 0$ , the slow eigenvectors include expressions  $B_x c_{s'} / (c_s^2 - b_v^2)$  and  $c_s^2 / (c_s^2 - b_x^2)$  which are of the form  $0/0$ . This singularity can be removed by using the following identities:

$$c_s = \frac{a|h_x|}{c_f}, \quad (35)$$

$$c_s^2 - b_v^2 = -\frac{b_x^2(b_y^2 + b_z^2)}{c_f^2 - b_x^2}. \quad (36)$$

For example,

$$\frac{b_y b_x c_s}{c_s^2 - b_x^2} = -\frac{a}{c_f} \frac{c_f^2 - b_x^2}{b_y^2 + b_z^2} \operatorname{sgn}(B_x) b_y, \quad (37)$$

$$\frac{b_y c_s^2}{\rho^{1/2}(c_s^2 - b_x^2)} = -\frac{a^2}{c_f^2} \frac{b_y}{\rho^{1/2}} \frac{c_f^2 - b_x^2}{b_y^2 + b_z^2}. \quad (38)$$

At  $B_x = 0$ , the slow eigenvectors can be defined as limiting values of  $B_x \rightarrow 0$ . Since we have a pair of slow eigenvectors,  $R_{u-c_s}$  and  $R_{u+c_s}$ , the resulting set is independent of whether  $B_x \rightarrow 0^+$  or  $B_x \rightarrow 0^-$ . We choose to define  $\operatorname{sgn}(B_x \equiv 0) = 1$  in (37).

(2) As  $b_y^2 + b_z^2$  approaches zero, the terms involving  $B_v / (c^2 - b_x^2)$  and  $B_z / (c^2 - b_x^2)$  may tend to infinity. They also are not defined at the points where  $b_y^2 + b_z^2 = 0$  for the fast eigenvectors in the case  $a^2 < b_x^2$  or the slow eigenvectors in the case  $a^2 > b_x^2$  or both eigenvectors in the case  $a^2 = b_x^2$ . Furthermore, the determinant of the matrix with the eigenvectors (34) as its columns is proportional to  $(c_f^2 - c_s^2)^2$  which will tend to zero if both  $b_y^2 + b_z^2$  and  $a^2 - b_x^2$  approach zero.

To examine the behavior of the eigenvectors (34) near these points, it is convenient to introduce the following variables for  $b_y^2 + b_z^2 \neq 0$ :

$$\alpha_f = \frac{\sqrt{c_f^2 - b_x^2}}{\sqrt{c_f^2 - c_s^2}}, \quad (39)$$

$$\alpha_s = \frac{1}{|b_x|} \frac{\sqrt{b_x^2 - c_s^2}}{\sqrt{c_f^2 - c_s^2}} = \frac{\sqrt{c_f^2 - a^2}}{\sqrt{c_f^2 - c_s^2}} \frac{1}{c_f}, \quad (40)$$

$$\beta_y = \frac{B_y}{\sqrt{b_y^2 + b_z^2}}, \quad (41)$$

$$\beta_z = \frac{B_z}{\sqrt{b_y^2 + b_z^2}}. \quad (42)$$

In these variables the expressions of the form (37), (38) for the slow eigenvectors, and similar expressions for the fast eigenvectors, are multiples of  $\alpha_f/\alpha_s$  and  $\alpha_s/\alpha_f$ , respectively. The determinant of the matrix with these eigenvectors as its columns is proportional to  $(b_y^2 + b_z^2)/(\alpha_f^2 \alpha_s^2)$ . Therefore, by multiplying the fast, slow, and Alfvén eigenvectors in (34) by  $\alpha_f$ ,  $\alpha_s$ , and  $1/\sqrt{b_y^2 + b_z^2}$ , respectively, we obtain a set of right eigenvectors which is well defined everywhere. For example, multiplication of expressions (37) and (38) by  $\alpha_s$  gives

$$\alpha_s \frac{b_y b_x c_s}{\rho(c_x^2 - b_x^2)} = -\frac{a}{c_f} \beta_y \alpha_f \text{sgn}(B_x), \quad (43)$$

$$\alpha_s \frac{b_y c_s^2}{\rho^{1/2}(c_s^2 - b_x^2)} = -\frac{a^2}{c_f^2} \frac{\beta_y}{\rho^{1/2}} \alpha_f. \quad (44)$$

At points where  $B_y^2 + B_z^2 = 0$ , we define  $\beta$ 's as some limiting values of (41)–(42), i.e.,

$$\beta_y = \beta_z = \frac{1}{\sqrt{2}}, \quad \text{if } B_y^2 + B_z^2 = 0. \quad (45)$$

Similarly, for  $\alpha$ 's, we define

$$\alpha_f = 1, \quad \alpha_s = 1, \quad \text{if } B_y^2 + B_z^2 = 0 \quad \text{and} \quad a^2 - b_x^2 = 0. \quad (46)$$

Note that with the above normalization either  $B_y c/(c^2 - b_x^2)$  or  $B_z c/(c^2 - b_x^2)$  are not continuous as both  $B_y$  and  $B_z$  approach zero. For them to be continuous, one can multiply slow (if  $a^2 > b_x^2$ ) or fast (if  $a^2 < b_x^2$ ) eigenvectors by the sign of the transverse magnetic field, which we define as 1, if  $B_y > 0$  or both  $B_y = 0$  and  $B_z > 0$ , and  $-1$ , if  $B_y < 0$  or both  $B_y = 0$  and  $B_z < 0$ . This step is not important for the Roe construction since the difference is only in the sign of the eigenvectors. On the other hand, as we will show in Section 6, it is crucial to have continuous fast (if  $a^2 < b_x^2$ ) and slow (if  $a^2 > b_x^2$ ) eigenvectors for the proper classification of the MHD characteristic fields.

#### IV.4. Decomposition Coefficients

Decomposition coefficients  $C_k$ 's are obtained by solving directly the following system of linear equations:

$$U_{i+1} - U_i = \sum_k C_k^{i+1/2} R_k^{i+1/2}. \quad (47)$$

Define

$$d_{1,5} = C_7 \pm C_1, \quad (48)$$

$$d_{2,4} = C_5 \pm C_3, \quad (49)$$

$$d_{6,7} = C_2 \pm C_6, \quad (50)$$

then the system decouples as follows.

The second, third, and fifth equations of (47) form the following system of equations for  $d_4$ ,  $d_5$ , and  $d_7$ :

$$\begin{pmatrix} \alpha_f c_f & \alpha_s c_s & 0 \\ -\beta_x \alpha_s b_x c_f & \beta_y \alpha_s \operatorname{sgn}(B_x)/c_f & -\beta_z \operatorname{sgn}(B_x) \\ -\beta_z \alpha_s b_x c_f & \beta_x \alpha_s \operatorname{sgn}(B_x)/c_f & \beta_y \operatorname{sgn}(B_x) \end{pmatrix} \begin{pmatrix} d_5 \\ d_4 \\ d_7 \end{pmatrix} = \rho^* \begin{pmatrix} \Delta u \\ \Delta v \\ \Delta w \end{pmatrix}, \quad (51)$$

where  $\alpha$ 's and  $\beta$ 's are defined by (39)–(42) and  $\Delta u = u_{i+1} - u_i$ , etc. The equations number four, six, and seven of (47) contain only  $d_1$ ,  $d_2$ , and  $d_6$ :

$$\begin{pmatrix} \alpha_s \beta_y c_f^2 / \rho^{1/2} & -\alpha_f a^2 \beta_y / (c_f^2 \rho^{1/2}) & \beta_z / \rho^{1/2} \\ \alpha_s \beta_z c_f^2 / \rho^{1/2} & -\alpha_f a^2 \beta_z / (c_f^2 \rho^{1/2}) & -\beta_y / \rho^{1/2} \\ \alpha_f \frac{c_f^2}{\gamma-1} + \alpha_s \frac{\gamma-2}{\gamma-1} c_f^2 & \alpha_s \frac{b_x^2 a^2}{c_f^2 (\gamma-1)} + \alpha_f \frac{\gamma-2}{\gamma-1} \frac{a^2}{c_f^2} & 0 \end{pmatrix} \begin{pmatrix} d_1 \\ d_2 \\ d_6 \end{pmatrix} = \begin{pmatrix} \Delta B_y \\ \Delta B_z \\ A \left( \frac{p}{\gamma-1} - \frac{B_y^2 + B_z^2}{2} \right) \end{pmatrix}. \quad (52)$$

By solving (51) and (52), we obtain the  $d$ 's. Then we obtain  $C_4$  from the first equation of (47),

$$C_4 = A\rho - \alpha_f d_1 - \alpha_s d_2, \quad (53)$$

and the rest of the coefficients from (48)–(50).

## V. NUMERICAL EXAMPLE

For the numerical example, we choose a coplanar MHD Riemann problem, which is an initial value problem with the initial data consisting of two constant states  $U_l$  and  $U_r$ . In our case, the initial left and right states are, respectively,  $\rho_l = 1$ ,  $u_l = 0$ ,  $v_l = 0$ ,  $p_l = 1$ ,  $(B_y)_l = 1$ ; and  $\rho_r = 0.125$ ,  $u_r = 0$ ,  $v_r = 0$ ,  $p_r = 0.1$ ,  $(B_y)_r = -1$ . In addition,  $B_z \equiv 0.75$  and  $\gamma = 2$ . Note that the initial hydrodynamical data used here are identical to those in Sod's shock tube problem [12].

Numerical solutions which were obtained for 800 grid points with  $\Delta x = 1$  and  $\Delta t = 0.2$  ( $\text{CFL} \sim 0.8$ ) are shown after 400 time steps unless specified otherwise. Initial discontinuity is located in the middle of the computational interval. The problem was solved by several numerical schemes including the newly constructed second-order Roe-type scheme, which was extended to second order by Harten's approach [8], the Lax–Friedrichs scheme [13], the Lax–Wendroff scheme with Lapidus-type viscosity [14]–[15], and the FCT scheme [16].

Figure 2 shows the results for the second-order upwind scheme using the Roe matrix in the form of  $A(V)$  with  $V$  given by (26) and (28)–(30). The solution consists of the following waves separated by constant states. The waves moving to the left are a fast rarefaction wave, denoted by FR in the figure, and a slow compound wave, denoted by SM. The waves moving to the right include a contact discontinuity, denoted by C, a slow shock (SS), and a fast rarefaction wave, FR. The solution was checked by calculating Riemann invariants across the rarefaction

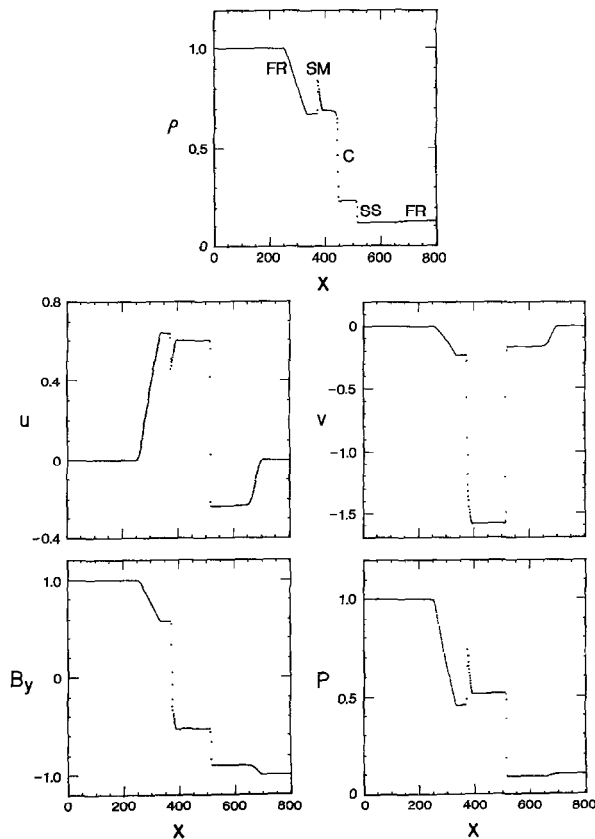


FIG. 2. Second-order upwind scheme.

waves and Rankine–Hugoniot jump conditions across the shock waves. The existence of a compound wave is due to the nonconvexity of the MHD equations and will be discussed in the next section.

We have also solved the problem by another second-order upwind scheme, where simple arithmetic averages of the density, velocity, full pressure, and magnetic field were used in constructing  $A_{i+1/2}$  in (14) in the form of  $A(W(U_i, U_{i+1}))$  as discussed in Section 4. The constant states obtained by this scheme and the ones obtained in the previous case are constant up to 4 significant digits, and they are the same for both schemes. In the transition regions the two schemes agree up to 2 significant digits.

Figure 3 represents the results for the two-step Lax–Wendroff scheme with Lapidus-type viscosity. There is an undershoot at the tail of the rarefaction wave. The shock is resolved with 4–5 transition points. Oscillations occur between fast rarefaction and slow compound wave, and between slow compound wave and a

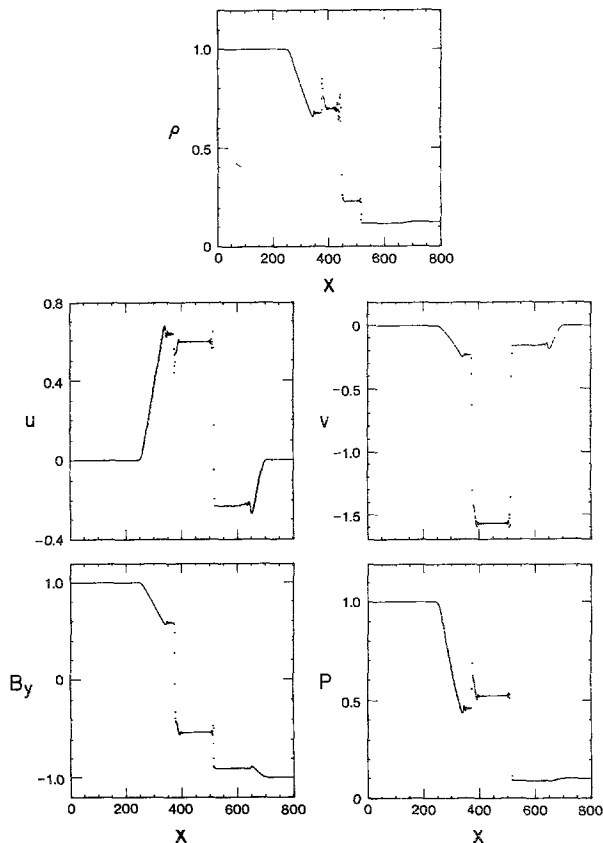


FIG. 3. Lax–Wendroff scheme with Lapidus-type viscosity.

contact. The contact discontinuity is resolved with 10–15 points. There is a slight overshoot at the right moving slow shock which is resolved with 5–8 points.

We have also tried to use the Lax–Wendroff scheme for the Riemann problem with the data identical to the above, except  $(B_y)_r = -0.4$ . For this case, the solution obtained by the upwind scheme or the Lax–Friedrichs scheme contains an almost stationary slow intermediate shock where the magnetic field changes its sign. However, with the Lax–Wendroff scheme we were not able to make numerical solutions stable with any value of artificial viscosity.

Figure 4 shows the results obtained by the first-order Lax–Friedrichs scheme. At the time shown, the constant states between the left moving fast rarefaction and the slow compound wave, and between the contact and the right moving slow shock are not yet realized. The slow shock is smeared by about 20 transition points. In order to demonstrate convergence of the Lax–Friedrichs scheme to the same solution as the one obtained by the second-order schemes, we have increased the

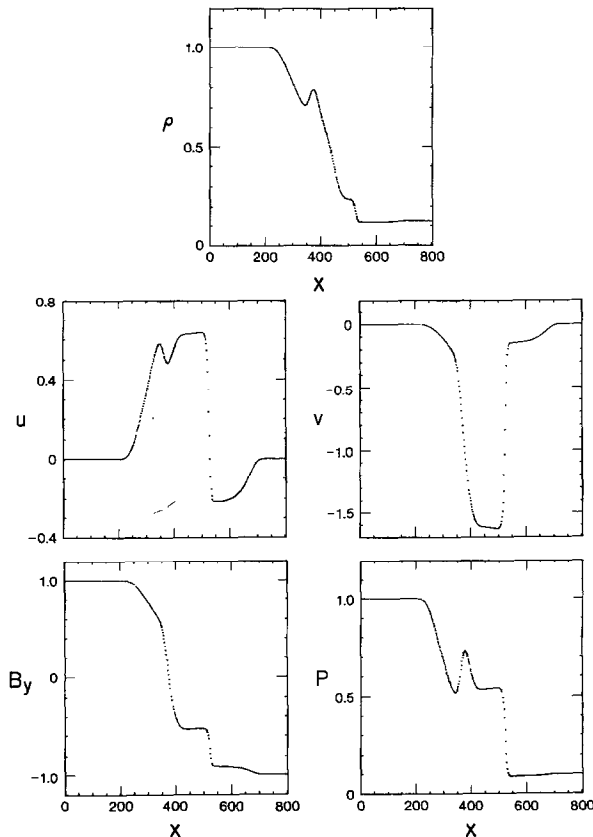


FIG. 4. Lax–Friedrichs scheme.

number of the grid points and the number of the time steps up to 20,000 and 10,000, respectively. The results are shown in Fig. 5. When drawn on the same scale, they coincide with the results obtained by the second-order upwind schemes, except the contact is resolved sharper by the upwind schemes. This may be due to the fact that in the upwind scheme, artificial compression was applied for the linearly degenerate field.

Figure 6 shows the results for the FCT method [17] after 800 time steps with  $\Delta t = 0.1$ . The CFL number used in the calculation is about 0.4, as suggested in [2]. (Even a smaller CFL number does not improve the results.) There is an undershoot at the tail of the rarefaction wave and at the contact discontinuity. Oscillations cover the constant states between the contact and the compound wave and between the slow and the fast waves moving to the right. The discontinuities are resolved sharply with few transition points. The same case, when run with CFL number 0.8,

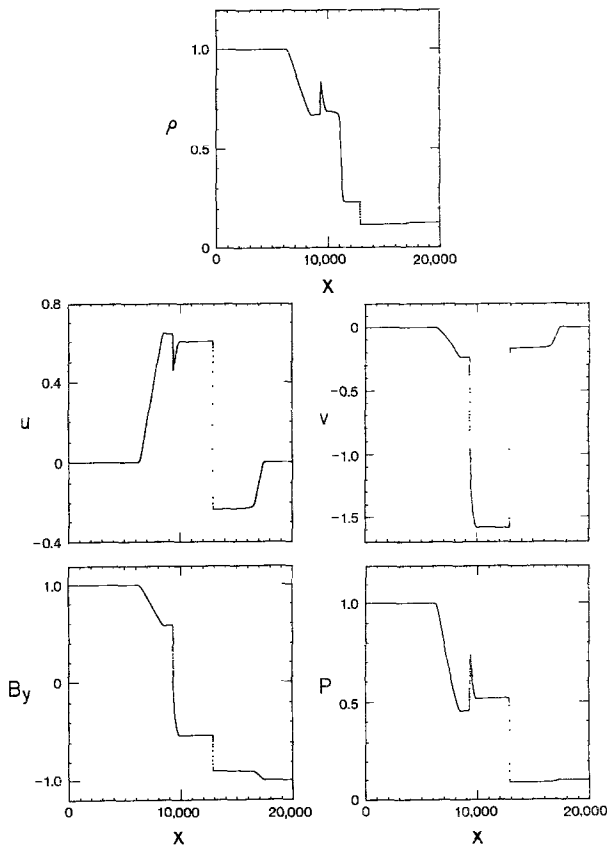


FIG. 5. Lax-Friedrichs scheme with 20,000 points and after 10,000 time steps.



increases drastically the oscillations between the left and the right-moving slow waves and also produces oscillations near the right-moving fast rarefaction wave.

In order to demonstrate the robustness of the upwind scheme for high Mach number problems, we have solved the same Riemann problem as above, but  $B_x \equiv 0$  and  $\rho_1 = 1000$ . The problem becomes a standard hydrodynamical Riemann problem if one replaces the plasma pressure by the sum of the plasma and the magnetic pressures. The exact solution (continuous line) and the numerical solution (dotted line) are shown in Fig. 7. The Mach number corresponding to the right-moving shock wave is 15.5. The amount of artificial compression used at the tangential discontinuity as prescribed by Harten [8] does not prevent the tangential discontinuity from spreading. On the other hand, artificial compression together with the second-order correction term causes the undershoot in the density profile near the tangential discontinuity. This undershoot diffuses in time.

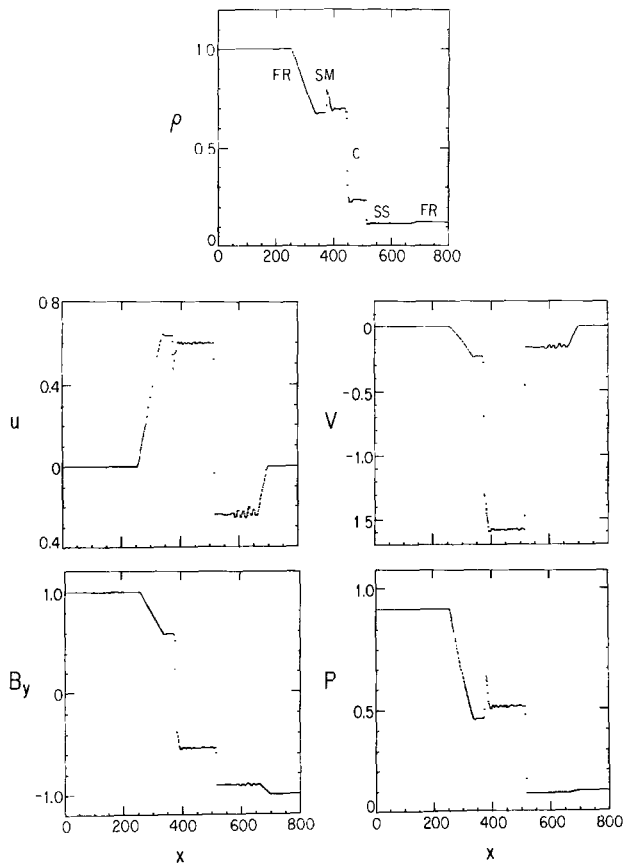


FIG. 6. FCT scheme.

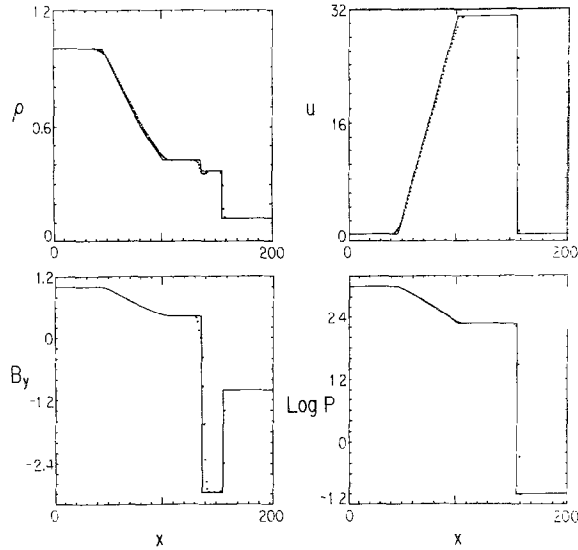


FIG. 7. High Mach number Riemann problem by second-order upwind scheme.

## VI. NONCONVEXITY OF THE MHD EQUATIONS

In this section, using the complete set of right eigenvectors constructed in Section 3, we will prove that the MHD equations are nonconvex. The following terminology is used: A pair  $(\lambda_k, R_k)$  is called the  $k$ th characteristic field where  $\lambda_k$  and  $R_k$  represent the  $k$ th eigenvalue and the corresponding eigenvector of the Jacobian matrix. As first shown by Bazer and Ericson [18], for a given left state the jump relations can be resolved for the right state and the shock speed by using the transverse magnetic field as a parameter. This one-parameter family of right states which can be connected by a shock to a given left state is called a shock curve. Following Lax [13], the  $k$ th characteristic field is called genuinely nonlinear if the appropriate eigenvalue is monotonic along the shock curve

$$\frac{d\lambda_k(u)}{d\varepsilon} = (\nabla_u \lambda_k) \cdot \frac{du}{d\varepsilon} \Big|_{\varepsilon=0} = (\nabla_u \lambda_k) \cdot R_k \neq 0, \quad (53)$$

where  $\varepsilon$  is the parameter along the shock curve. A characteristic field such that  $(\nabla_u \lambda_k) \cdot R_k \equiv 0$  identically along the shock curve is called linearly degenerate. For example, sound waves in Euler equations represent genuinely nonlinear fields and the contact discontinuity represents a linearly degenerate field. Such systems of conservation laws, such as Euler equations, with all of the characteristic fields being either genuinely nonlinear or linearly degenerate are called convex.

Using the set of right eigenvectors constructed in Section 3,  $(\nabla \lambda) \cdot R$  is propor-

tional to  $B_y$ , near  $B_y = 0$  for the MHD fast wave if  $a^2 < b_x^2$ , and the slow wave if  $a^2 > b_x^2$ . (We assume here that  $B_z = 0$  since MHD shocks are coplanar.) Thus these fields, whose  $(\nabla\lambda) \cdot R$  is zero at one point where  $B_y = 0$  and nonzero elsewhere, are neither linearly degenerate nor genuinely nonlinear. Therefore, the MHD system is nonconvex! (Note that by using the set of right eigenvectors (34) as given, it follows that  $(\nabla\lambda) \cdot R$  is nonzero for both slow and fast waves and that they are genuinely nonlinear, see Jeffrey and Taniuti [6]. But this conclusion is not correct, since the set (34) is not complete.)

Nonconvexity can also be derived from the direct approach used by Bazer and Ericson (18) to study the variations of different quantities along the shock curve by using  $(B_y)_r$  as a parameter. In particular, they showed that the fast (slow) eigenvalue curve will intersect the shock speed ( $s$ ) curve if  $a^2 < b_x^2$  ( $a^2 > b_x^2$ ), and  $ds/d(B_y)_r = 0$  at the intersection point. To illustrate this approach, consider the following simple example. Assume the transverse magnetic field to be small,  $(B_y)_l$  is given and  $(B_y)_r$  is a parameter along the shock curve. Without loss of generality, we can set  $\rho_l = 1$ ,  $u_l = 0$ ,  $B_x \equiv 1$ , and consider a case with  $\gamma = 2$ ,  $p_l = 1$ . Expanding the Rankine-Hugoniot jump relations using  $(B_y)_r$  as a parameter [18], we obtain

$$\lambda_r = (u - c_s)_r = -1 + \frac{3(B_y)_r^2 - (B_y)_l^2}{4} + \dots, \quad (54)$$

$$s = -1 + \frac{(B_y)_r^2 + (B_y)_r(B_y)_l}{4} + \dots, \quad (55)$$

and  $\lambda_l = -1 + \frac{1}{2}(B_y)_l^2 + \dots$ , and  $(B_y)_r^2 \leq (B_y)_l^2$ . This implies that both  $\lambda_r$  and  $s$  curves intersect at  $(B_y)_r = -(B_y)_l/2$ , and  $ds/d(B_y)_r = 0$  at this point. Also, since the shock speed is equal to the characteristic speed at the intersection point, a rarefaction wave can be attached to a shock there.

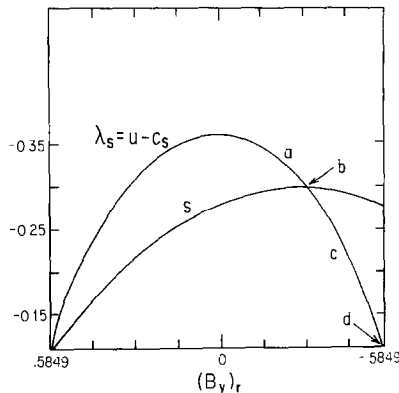


FIG. 8. Dependence of the shock ( $s$ ) and the slow characteristic speeds ( $\lambda_s$ ) on the variable  $(B_y)_r$ .

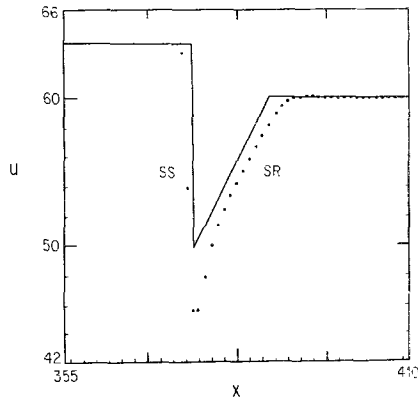


FIG. 9. Slow compound wave ( $x$ -component of velocity). The continuous line shows the position of the slow shock and attached to it rarefaction wave obtained by resolving the Rankine-Hugoniot jump relations and the Riemann invariants. The dotted line denotes values obtained from the numerical calculation.

To illustrate the global behavior of the eigenvalue along the shock curve, we consider the compound wave in the first numerical example of the previous section. Using the numerical data for the left state with respect to the slow shock ( $\rho = 0.6763$ ,  $u = 0.6366$ ,  $v = -0.2333$ ,  $B_y = 0.5849$ ,  $p = 0.4574$ ), we have resolved jump relations using  $(B_y)_r$  as a parameter. The dependence of the shock speed ( $s$ ) and the slow characteristic speed ( $u - c_s$ ) with respect to  $(B_y)_r$  is shown in Fig. 8 for the entropy nondecreasing shocks. Point ( $b$ ) denotes the intersection of these two curves. The values of the variables at the intersection point are as follows:  $\rho = 0.7935$ ,  $u = 0.4983$ ,  $v = -1.290$ ,  $B_y = -0.3073$ ,  $p = 0.6687$ , and  $s = -0.2995$ .

The portion of the solution containing the compound wave of a slow shock (SS) and attached to it a rarefaction wave (SR) is shown in Fig. 9 for the  $u$  variable. The continuous line in the figure represents an analytical solution of the compound wave in which the rarefaction wave is obtained through Riemann invariants with the head of the rarefaction wave specified at the intersection point. Then the values at the tail of the rarefaction are as follows:  $\rho = 0.6965$ ,  $u = 0.5987$ ,  $v = -1.583$ ,  $B_y = -0.5341$ , and  $p = 0.5157$ . For comparison, the values at the tail obtained numerically by the second-order upwind scheme as shown with the dotted line in the figure are  $\rho = 0.6963$ ,  $u = 0.5997$ ,  $v = -1.578$ ,  $B_y = -0.5341$ , and  $p = 0.5133$ . The agreement is excellent.

The relationship between the shock speed ( $s$ ) and the characteristic speeds ( $\lambda$ ) for the different points  $a$ ,  $b$ ,  $c$ , and  $d$  on the shock curve in Fig. 8 is illustrated in the  $(x, t)$  diagrams in Fig. 10. The first case ( $a$ ) illustrates the shock with convergent slow characteristics and is similar to the shocks encountered for the Euler equations which correspond to genuinely nonlinear fields. In the second case ( $b$ ), the right slow characteristic speed is equal to the shock speed. This allows for a rarefaction wave to be attached to such a shock as in the compound wave considered in the

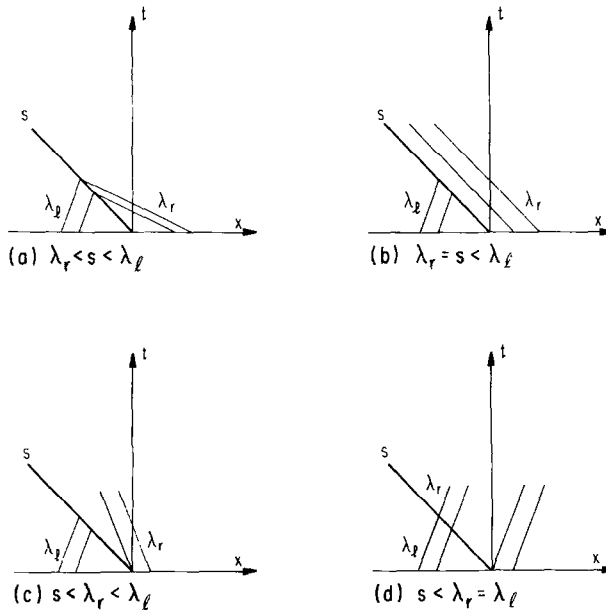


FIG. 10. Relationship between the shock ( $s$ ) and the slow characteristic speeds ( $\lambda$ ) for the different points along the shock curve in Fig. 8.

above numerical example. Case (c) shows a shock having a divergent slow characteristic on the right-hand side. In this case, two waves of the same family can travel in the same direction without one being overtaken by another. The last diagram (d) shows a particular case of the previous one in which the characteristic speed is constant across the shock. It corresponds to a  $180^\circ$  Alfvén wave, namely, density, pressure,  $x$ -component of the velocity are constant across the shock and the transverse magnetic field reverses its sign.

Note that since  $B_y$  changes its sign across the slow shock in the compound wave, the shock is an intermediate shock. If we believe in the usual argument that MHD intermediate shocks are not admissible [6, 19], then we may conclude that all numerical schemes tested in Section 5 admit nonphysical shocks. This would be a serious problem in numerical magnetohydrodynamics. However, contrary to this belief, it has recently been shown by numerical solutions of resistive MHD equations that at least some types of intermediate shocks, including the one here, can exist [20]. Specifically, it was shown that some intermediate shocks can be created by a steepening process from a continuous wave.

## VII. DISCUSSION AND CONCLUSION

In this paper we have shown a procedure to construct a Roe-type upwind differencing scheme for the one-dimensional MHD equations. Numerical experiments

demonstrate that the scheme has several advantages in comparison with the standard schemes, such as nonoscillatory behavior, and high resolution of discontinuities. In addition, based on our experience with a Roe scheme, either for the Euler equation or the MHD equations, the scheme is nonlinearly stable. Since there are multiple time scales in MHD, one may have a further advantage to use the upwind scheme. Because the scheme is based on linear decomposition of characteristic fields, one can treat each field separately. In the case that the short time scale phenomenon is not important, one can modify the scheme by slowing down the fast characteristic speeds explicitly or treating it implicitly, so that a large time step size can be used.

Although the upwind scheme for the MHD equations is a straightforward extension of the scheme for the Euler equations. The construction is quite involved. The scheme requires about 10 times more floating point operations per grid point per time step than the Lax–Wendroff scheme. However, because of its many advantages over other schemes, the effort is worthwhile in some cases. Due to its high resolution of discontinuities, one can use the upwind scheme with fewer grid points. For example, in the first numerical example in Section 5, one can use the upwind scheme with 200 grid points instead of 800 points and still obtain a reasonable result. By using 200 grid points and thus reducing the number of time steps by 4, the upwind wind scheme becomes more efficient than the Lax–Wendroff scheme with 800 grid points. Most importantly, since the upwind scheme does not produce non-physical oscillations, it is easier to understand the computational results. For example, the nonconvexity of the MHD equations was first discovered by using the upwind scheme for the first numerical example in the paper. With the Lax–Wendroff scheme or the FCT scheme, one could have trouble identifying the compound wave in the solution, because of the numerical oscillation; for the Lax–Friedrichs scheme, it requires too many grid points.

In the paper, we have also proved rigorously the nonconvex property by using our complete set of right eigenvectors. One consequence is that compound waves can exist in MHD. Since it is only now that we know that the MHD equations are nonconvex, further research is required to clarify their solutions and their relations to various admissibility criteria.

#### ACKNOWLEDGMENTS

It is a pleasure to acknowledge valuable discussions with Drs. F. V. Coroniti, B. Engquist, A. Harten, and S. Osher. This work was supported by the National Science Foundation Grant ATM 85–21125, by U. S. Department of Energy Grant DE-FG03–86ER 53225 and by a grant from the California Space Institute.

#### REFERENCES

1. A. HARTEN, P. D. LAX, AND B. VAN LEER, *SIAM Rev.* **25**, 35 (1983).
2. P. WOODWARD AND P. COLELLA, *J. Comput. Phys.* **54**, 115 (1984).

3. P. L. ROE, *J. Comput. Phys.* **43**, 357 (1981).
4. S. K. GODUNOV, *Math. Sb.* **47** 271 (1959).
5. S. OSHER AND F. SOLOMON, *Math. Comput.* **38**, 339 (1982).
6. A. JEFFREY AND T. TANIUTI, *Non-linear Wave Propagation* (Academic Press, New York, 1964).
7. P. GARABEDIAN, *Partial Differential Equations* (Wiley, New York, 1964).
8. A. HARTEN, *J. Comput. Phys.* **49**, 357 (1983).
9. S. OSHER AND S. CHAKRAVARTHY, *J. Comput. Phys.* **50**, 447 (1983).
10. A. HARTEN AND J. M. HYMAN, *J. Comput. Phys.* **50**, 235 (1983).
11. M. BRIO, Ph.D. dissertation, Univ. of California, Los Angeles, 1984 (unpublished).
12. G. SOD, *J. Comput. Phys.* **27**, 1 (1978).
13. P. D. LAX, *Comm. Pure Appl. Math.* **7**, 159 (1954).
14. P. D. LAX AND B. WENDROFF, *Comm. Pure Appl. Math.* **13**, 217 (1960).
15. A. LAPIDUS, *J. Comput. Phys.* **2**, 154 (1967).
16. J. P. BORIS AND D. L. BOOK, *J. Comput. Phys.* **11**, 38 (1973).
17. J. P. BORIS, N.R.L. Memorandum Report 3237, 1976 (unpublished).
18. J. BAZER AND W. B. ERICSON, *Astrophys. J.* **129**, 758 (1959).
19. A. R. KANTROWITZ AND H. E. PETSCHEK, *Plasma Physics in Theory and Application*, edited by W. B. Kunkel (McGraw-Hill, New York, 1966.)
20. C. C. WU, *Geophys. Res. Lett.* **14**, 668 (1987).